Inorg. Chem. **2002**, *41*, 321–330

3,3′-Bis(triphenylsilyl)biphenoxide as a Sterically Hindered Ligand on Fe(II), Fe(III), and Cr(II)

Ajay Kayal and Sonny C. Lee*

Department of Chemistry, Princeton University, Princeton, New Jersey 08544

Received August 16, 2001

The structural coordination chemistry of the sterically hindered 3,3′-bis(triphenylsilyl)-1,1′-bi-2-phenoxide ligand ($[^{TPS}LO_2]^{2-}$), an isosteric homologue of a chiral binaphthoxide ligand used in asymmetric induction, has been investigated on Fe(II), Fe(III), and Cr(II). The ligand diol ($^{TPS}L(OH)_2$, **2**) can be prepared on a multigram scale from 2,2′-dimethoxybiphenyl via a convenient, two-step ortho-metalation/silylation/deprotection sequence; the sodium salt of the ligand dianion ($Na_2[^{TPS}LO_2]$, **3**) can be obtained by NaH deprotonation and was crystallographically characterized with two THF ligands bound to each cation. Protonolysis of $Fe[N(SiMe_3)_2]_2$ or $Cr[N(SiMe_3)_2]_2(THF)_2$ with biphenol **2** in arene solvent gives $[Fe(\mu\text{-}^{TPS}LO_2)]_2$ (**4**) or $(^{TPS}LO_2)Cr(THF)_2$ (**9**), respectively, while anion metathesis of $FeCl_2$ or $FeCl_3$/bipy with biphenoxide salt **3** in THF yields $(^{TPS}LO_2)Fe(THF)_2$ (**8**) or ferric monomer $(^{TPS}LO_2)FeCl$-(bipy) (**10**), respectively. Dimer **4** reacts with exogenous ligands to form monomeric ligand adducts of Fe(II): with py, $(^{TPS}LO_2)Fe(py)_2$ (**5**); with bipy, $(^{TPS}LO_2)Fe(bipy)$ (**6**); with XyNC (Xy = 2,6-xylyl), $(^{TPS}LO_2)Fe(CNXy)_4$ (**7**); and with THF, **8**. Complexes were characterized in solution by ^1H NMR and in the solid state by single-crystal X-ray diffraction. The 4-coordinate complexes (**5**, **6**, **8**, **9**) adopt skew-distorted tetrahedral (for Fe(II)) or square planar (for Cr(II)) geometries; the 5- and 6-coordinate complexes (**10** and **7**) assume more typical distorted square pyramidal/trigonal bipyramidal and cis-octahedral stereochemistries. Dimer **4** possesses an unusual structure where each Fe(II) center is pseudo-4-coordinate and each biphenoxide ligand provides one terminal phenoxide donor, one bridging phenoxide, and a weak aromatic π-interaction from one of the phenyl groups of a $SiPh_3$ substituent. The steric influence of the hindered biphenoxide ligand within the coordination sphere is revealed structurally through distortion of coordination polyhedra in the 4-coordinate species and through conformational and deformational changes within the biphenoxide ligand itself.

Introduction

1,1′-Bi-2-aryloxides are useful ancillary ligands for the control of metal-based reactivity.[1−3] As a bidentate, dianionic chelate, the biaryloxy scaffold offers two intrinsic features that can be exploited to control metal geometry. First, the requisite torsion of the aryl−aryl linkage forces a distinctly nonplanar 7-membered metallacycle upon coordination; this geometry creates a pronounced C_2 chiral axis of proven value for asymmetric induction.[1] Second, the ring positions (3,3′) adjacent to the coordinating oxygen atoms allow for facile incorporation[4] of forward-directed substituents to shape the metal coordination sphere; substituents of high steric demand should promote stereochemically rigid environments.

Biaryloxides with very hindered 3,3′-substituents are therefore intriguing as potential geometry constraining ligands. Of the various substituents reported to date, the triphenylsilyl group shows promise in this regard based on chemistry developed from the 3,3′-bis(triphenylsilyl)-1,1′-bi-2-naphthoxide ligand. This biaryloxide derivative has served as a chiral auxiliary on Al(III) to mediate enantioselective radical cyclizations[5] and catalyze asymmetric Diels−Alder,[6] ene,[7] and Claisen reactions;[8] the latter transformations in particular give excellent diastereo- and enantioselectivities under appropriate conditions.[6−8] For d- and

* Author to whom correspondence should be addressed. E-mail: sclee@princeton.edu.

(1) Pu, L. *Chem. Rev.* **1998**, *98*, 2405 and references therein.
(2) Eilerts, N. W.; Heppert, J. A. *Polyhedron* **1995**, *14*, 3255.
(3) Kayal, A.; Ducruet, A. F.; Lee, S. C. *Inorg. Chem.* **2000**, *39*, 3696 and references therein.
(4) (a) Gschwend, H. W.; Rodriguez, H. R. *Org. React. (N.Y.)* **1979**, *26*, 1. (b) Beak, P.; Snieckus, V. *Acc. Chem. Res.* **1982**, *15*, 306. (c) Snieckus, V. *Chem. Rev.* **1990**, *90*, 879.
(5) Nishida, M.; Hayashi, H.; Nishida, A.; Kawahara, N. *Chem. Commun.* **1996**, 579.

10.1021/ic010909y CCC: $22.00
Published on Web 01/03/2002

Scheme 1

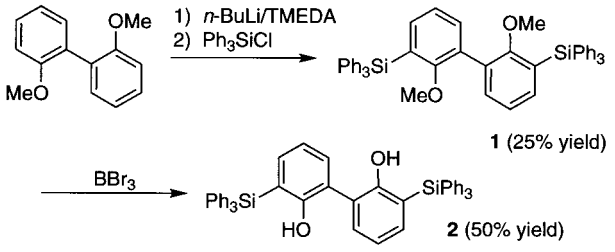

f-elements, complexes with this ancillary ligand are known for La(III),[9] Ti(IV),[10] Zr(IV),[10] and Ta(V).[11] These high-valent, early metal complexes show well-defined solution chemistry, resist ligand disproportionation, and, for the titanium and zirconium species,[10] catalyze stereoselective olefin polymerization and alkyne trimerization. All previous studies with this chelate have emphasized metal-centered reaction chemistry but, with one exception,[11] have left its structural chemistry largely unaddressed. To better define the influence of this hindered ligand type on metal geometry, we present here a comparative structural investigation of the coordination chemistry of the biphenoxide homologue, 3,3′-bis(triphenylsilyl)-1,1′-bi-2-phenoxide ($[^{TPS}LO_2]^{2-}$), as a ligand on Fe(II), Fe(III), and Cr(II).

Results

Ligand Synthesis. The 3,3′-bis(triphenylsilyl) derivatives of biphenol and binaphthol can be obtained in good yields by a multistep protocol where the *o*-silyl substituents are incorporated via 1,3-rearrangements of metalated silyl ethers.[12] We have found that direct ortho-metalation and silylation of commercial 2,2′-dimethoxybiphenyl,[13] followed by BBr_3 deprotection of the resultant hindered bianisole **1**, provide a simpler alternative route to the desired 3,3′-bis(triphenylsilyl)-1,1′-bi-2-phenol ($^{TPS}L(OH)_2$, **2**) (Scheme 1). Although yields are limited[14] by incomplete silylation at the first stage and competing ipso-borodesilylation[15] chemistry during deprotection, our present synthesis has the virtue of experimental convenience, easily affording >10 g quantities of pure product at both steps through simple recrystallizations. The ligand dianion can be obtained as the disodium salt **3** by treatment of biphenol **2** with excess NaH in THF (see Scheme 2).

Coordination Chemistry and Solution Characterization. The metal chemistry of the $[^{TPS}LO_2]^{2-}$ ligand presented herein is summarized in Scheme 2. Ligand substitution reactions involving complexes of the hindered biphenoxide are marked by conspicuous color changes, as noted in the scheme.

The protonolysis of $Fe[N(SiMe_3)_2]_2$[16] with 1 equiv of ligand diol **2** affords the chelated ferrous dimer $[Fe(\mu\text{-}^{TPS}LO_2)]_2$ (**4**) in good yield. Dimer **4** reacts smoothly with exogenous ligands and serves as a practical entry point to the coordination chemistry of the monomeric $[(^{TPS}LO_2)Fe]$ fragment. Thus, treatment of complex **4** with pyridine, 2,2′-bipyridyl, and 2,6-dimethylphenylisonitrile (XyNC) generates the corresponding adducts $(^{TPS}LO_2)Fe(py)_2$ (**5**), $(^{TPS}LO_2)Fe(bipy)$ (**6**), and $(^{TPS}LO_2)Fe(CNXy)_4$ (**7**), respectively, while dissolution of **4** in THF leads to the immediate formation of the solvent adduct $(^{TPS}LO_2)Fe(THF)_2$ (**8**). Complex **8** is also available directly by treatment of $FeCl_2$ with 1 equiv of the biphenoxide salt **3** in THF. The bound THF ligands in complex **8** are labile, and dissolution in poorly coordinating solvents such as benzene or CH_2Cl_2 leads to the immediate formation of dimer **4**; this behavior occurs to a lesser extent for the bis(pyridine) adduct **5**, which slowly (over hours) converts to **4** in the same solvents unless excess pyridine is present.

All of the ferrous complexes (except THF-labile **8**) present well-defined ^1H NMR spectra in CD_2Cl_2 or C_6D_6 (see Experimental Section for NMR data), with solution molecular symmetries that fit the solid-state structures identified by X-ray diffraction. The spectra[17] of the 4-coordinate species (**5**, **6**) and the dimer (**4**) are marked by broad signal envelopes from the triphenylsilyl group and by a highly dispersed set (ca. 100 ppm) of ligand biphenyl backbone resonances consistent with the presence of high-spin Fe(II) centers;[18] the spectroscopic data for pyridine and bipyridyl coligands show similar dispersions but with one resonance missing in each, probably from broadening of the *o*-H signals. In contrast, isonitrile complex **7**, which is low-spin due to its strong-field ligand environment, displays sharp, well-resolved signals within the diamagnetic chemical shift range for all ligand protons.

In order to increase the structural diversity, biphenoxide complexes of Cr(II) and Fe(III) were also synthesized. Protonolysis of $Cr[N(SiMe_3)_2]_2(THF)_2$[19] with 1 equiv of biphenol **2** yields $(^{TPS}LO_2)Cr(THF)_2$ (**9**), the chromous

(6) (a) Maruoka, K.; Itoh, T.; Shirasaka, T.; Yamamoto, H. *J. Am. Chem. Soc.* **1988**, *110*, 310. (b) Maruoka, K.; Concepcion, A. B.; Yamamoto, H. *Bull. Chem. Soc. Jpn.* **1992**, *65*, 3501. (c) Bao, J.; Wulff, W. D.; Rheingold, A. L. *J. Am. Chem. Soc.* **1993**, *115*, 3814.
(7) Maruoka, K.; Hoshino, Y.; Shirasaka, T.; Yamamoto, H. *Tetrahedron Lett.* **1988**, *29*, 3967.
(8) Maruoka, K.; Banno, H.; Yamamoto, H. *J. Am. Chem. Soc.* **1990**, *112*, 7791.
(9) Schaverien, C. J.; Meijboom, N.; Orpen, A. G. *J. Chem. Soc., Chem. Commun.* **1992**, 124.
(10) van der Linden, A.; Schaverien, C. J.; Meijboom, N.; Ganter, C.; Orpen, A. G. *J. Am. Chem. Soc.* **1995**, *117*, 3008.
(11) Thorn, M. G.; Moses, J. E.; Fanwick, P. E.; Rothwell, I. P. *J. Chem. Soc., Dalton Trans.* **2000**, 2659.
(12) (a) Maruoka, K.; Itoh, T.; Araki, Y.; Shirasaka, T.; Yamamoto, H. *Bull. Chem. Soc. Jpn.* **1988**, *61*, 2975. (b) Buisman, G. J. H.; van der Veen, L.; Klootwijk, A.; de Lange, W. G. J.; Kamer, P. C. J.; van Leeuwen, P. W. N. M.; Vogt, D. *Organometallics* **1997**, *16*, 2929.
(13) A similar route involving the bis(methoxymethyl) ether of binaphthol has been reported: Cox, P. J.; Wang, W.; Snieckus, V. *Tetrahedron Lett.* **1992**, *33*, 2253.
(14) The undesired side reactions at both steps could probably be suppressed and conversions thereby improved through the use of a more potent directed metalation group.[4,13]
(15) (a) Sharp, M. J.; Cheng, W.; Snieckus, V. *Tetrahedron Lett.* **1987**, *28*, 5093. (b) Gross, U.; Kaufmann, D. *Chem. Ber.* **1987**, *120*, 901. (c) Kaufmann, D. *Chem. Ber.* **1987**, *120*, 853.
(16) (a) Anderson, R. A.; Faegri, K., Jr.; Green, J. C.; Haaland, A.; Lappert, M. F.; Leung, W.-P.; Rydpal, K. *Inorg. Chem.* **1988**, *27*, 1782. (b) Olmstead, M. M.; Power, P. P.; Shoner, S. C. *Inorg. Chem.* **1991**, *30*, 2547.
(17) Probable assignments for the paramagnetically shifted resonances were made by comparison of integral ratios and by correlations in chemical shifts for signals from related complexes **5** and **6**.
(18) Swift, T. J. The Paramagnetic Line Width. In *NMR of Paramagnetic Molecules*; La Mar, G. N., Horrocks, W. D., Jr., Holm, R. H., Eds.; Academic Press: New York, 1973.

Scheme 2

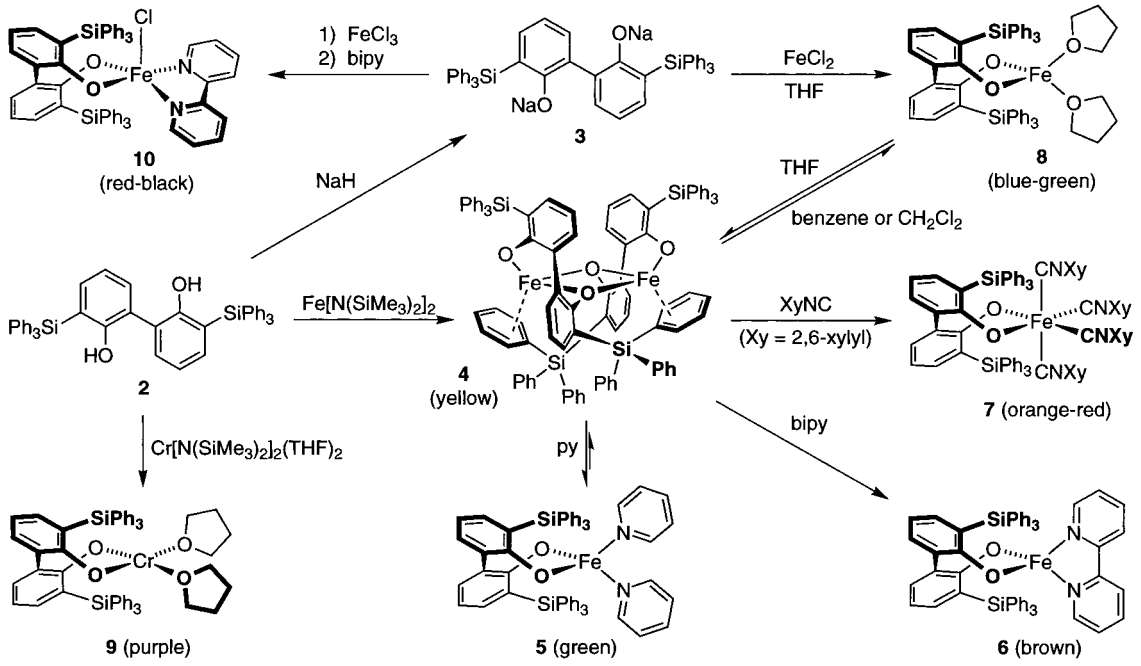

Table 1. Crystallographic Data[a] for $^{TPS}L(OH)_2$ (**2**), $[Na(THF)_2]_2(^{TPS}LO_2)\cdot 2THF$ ([**3**](THF)$_4$·2THF), $[Fe(\mu\text{-}^{TPS}LO_2)]_2\cdot 3C_6H_6$ (**4**·3C$_6$H$_6$), ($^{TPS}LO_2$)Fe(bipy) (**6**), ($^{TPS}LO_2$)Fe(CNXy)$_4$·(CH$_2$Cl$_2$/Et$_2$O) (**7**·(CH$_2$Cl$_2$/Et$_2$O)), ($^{TPS}LO_2$)M(THF)$_2$ (M = Fe/Cr: **8**/**9**), ($^{TPS}LO_2$)FeCl(bipy)·Et$_2$O·(THF/Et$_2$O) (**10**·Et$_2$O·(THF/Et$_2$O))

	2	[**3**](THF)$_4$·2THF	**4**·3C$_6$H$_6$	**6**	**7**·(CH$_2$Cl$_2$/Et$_2$O)	**8**	**9**	**10**·Et$_2$O ·THF
formula	$C_{48}H_{38}O_2Si_2$	$C_{72}H_{84}Na_2O_6Si_2$	$C_{114}H_{90}Fe_2O_4Si_4$	$C_{58}H_{44}FeN_2O_2Si_2$	$(C_{84}H_{72}FeN_4O_2Si_2)^b$	$C_{56}H_{52}FeO_4Si_2$	$C_{60}H_{60}Cl_8CrO_4Si_2$	$C_{66}H_{62}ClFeN_2O_4Si_2$
fw	702.96	1179.55	1747.92	912.98	(1281.49)^b	901.01	1236.86	1094.66
space group	$P\bar{1}$ (No. 2)	$P2_1/n$ (No. 14)	$P2_1/n$ (No. 14)	$C2/c$ (No. 15)	$P2_1/c$ (No. 14)	$P2_1/n$ (No. 14)	$P2_1/c$ (No. 14)	$P2_1/n$ (No. 14)
Z	2	4	4	2	4	4	4	4
a, Å	10.8073(6)	12.4304(5)	14.3710(5)	13.9516(7)	16.7731(6)	13.8422(6)	21.783(3)	12.8214(6)
b, Å	11.3587(7)	21.3410(6)	14.6800(4)	15.2681(6)	14.4705(3)	14.6838(7)	14.335(3)	29.735(2)
c, Å	18.596(1)	24.439(1)	44.681(2)	21.253(1)	33.678(1)	22.3321(6)	20.126(3)	15.7349(9)
α, deg	75.545(2)							
β, deg	73.936(3)	93.278(1)	92.670(1)	96.216(2)	99.991(1)	92.939(2)	109.541(7)	99.158(3)
γ, deg	62.598(2)							
V, Å^3	1927.4(2)	6472.5(4)	9416.0(6)	4500.6(4)	8050.1(4)	4533.2(3)	5922.6(2)	5922.3(6)
temp, K	200(2)	200(2)	200(2)	200(2)	200(2)	130(2)	200(2)	200(2)
θ_{max}, deg	27.35	22.53	23.30	27.53	22.46	25.00	22.47	22.48
ρ_{calcd}, g·cm^{-3}	1.21	1.21	1.23	1.35	(1.06)^b	1.32	1.39	1.29
μ, mm^{-1}	0.131	0.120	0.410	0.436	(0.262)^b	0.434	0.640	0.390
completeness of data, %	97.3	99.7	98.0	99.5	99.9	99.8	98.5	95.2
R (wR2),[c] %	5.89 (11.37)	8.55 (24.01)	5.53 (13.93)	5.22 (10.56)	5.23 (12.36)	5.12 (11.05)	8.44 (18.67)	4.97 (11.54)
S[d]	1.012	1.059	1.019	1.042	1.059	1.020	1.021	1.054

[a] Data collected with graphite-monochromatized Mo Kα radiation ($\lambda = 0.71703$ Å) using ω scans. [b] Calculated with exclusion of unresolved, compositionally disordered lattice solvent. [c] Calculated for $I > 2\sigma(I)$: $R = \sum||F_o| - |F_c||/\sum|F_o|$, wR2 = $\{\sum[w(F_o^2 - F_c^2)^2]/\sum[w(F_o^2)^2]\}^{1/2}$. [d] S = goodness of fit = $[\sum w(F_o^2 - F_c^2)^2/(n - p)]^{1/2}$, where n is the number of reflections and p is the number of parameters refined.

homologue to ferrous−THF complex **8**. The chromous complex is more sensitive to oxidation than its ferrous counterpart, but much less prone to decomposition by THF loss; the synthesis of **9**, in fact, is conducted in toluene with only stoichiometric amounts of THF supplied by the chromous amide starting material, and the product can be recrystallized without ligand loss from arene and CH_2Cl_2 solvents. The reaction of $FeCl_3$ with 1 equiv of biphenoxide salt **3** results in an immediate color change indicative of complex formation, although isolation attempts at this stage have given only uncharacterized powder. Addition of 1 equiv of 2,2′-bipyridyl to this solution, however, allows isolation of crystalline ($^{TPS}LO_2$)FeCl(bipy) (**10**) in limited yield. The ^{1}H NMR spectra of complexes **9** and **10** consist of very broad and uninformative resonances that are characteristic of high-spin Cr(II) and Fe(III).[18]

Structural Studies. Single-crystal X-ray diffraction analyses (Table 1) were used to establish definitive compound identities and to assess the structural influence of $[^{TPS}LO_2]^{2-}$ ligation in different coordination environments. For all

(19) (a) $Cr[N(SiMe_3)_2]_2(THF)_2$ was prepared by modification (see Experimental Section, General Considerations) of the literature procedure: Horvath, B.; Strutz, J.; Horvath, E. G. *Z. Anorg. Allg. Chem.* **1979**, *457*, 38. (b) Bradley, D. C.; Hursthouse, M. B.; Newing, C. W.; Welch, A. J. *J. Chem. Soc., Chem. Commun.* **1972**, 567.

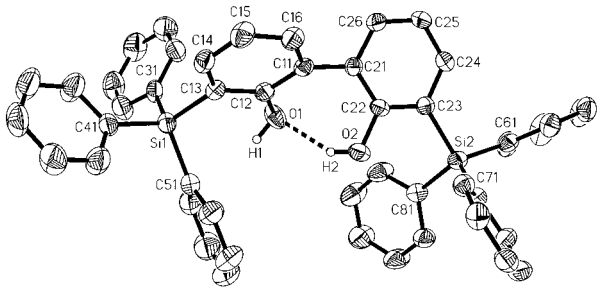

Figure 1. Structure of $^{TPS}L(OH)_2$ (**2**) with thermal ellipsoids (50% probability level) and selected atom labels; aryl hydrogen atoms are not shown. Selected distances (Å) and angles (deg): O(1)···O(2), 2.751(3); O(1)···H(2), 1.993(4); O−H, 0.84 (fixed); O(2)−H(2)···O(1), 149.7(5); dihedral angle between C(11−16) and C(21−26) planes (biphenyl torsion), 51.77(9).

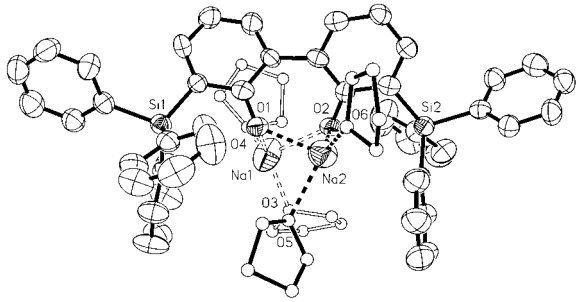

Figure 2. Structure of $[Na(THF)_2]_2[^{TPS}LO_2]$ ([**3**](THF)$_4$) with thermal ellipsoids (50% probability level) and selected atom labels; ball-and-stick representations are used for THF ligands, and hydrogen atoms are not shown. All THF ligands are disordered over two orientations, and only the major component for each is presented.

structures, the biphenoxy backbone is labeled consistently as indicated in Figure 1, with the exception of dimer **4**, where the second independent ligand is designated using [O10, C101−C106] and [O20, C201−C206] for its phenyl halves, and complex **6**, where a crystallographic 2-fold axis relates [O1, C11−C16] to [O1A, C11A−C16A].

(a) "Free" Ligand. The solid-state structure of biphenol **2** was determined in order to provide reference metrics for the uncomplexed ligand. The biphenol in this structure (Figure 1) possesses one internal hydrogen bond between phenol groups, as evidenced by the O1···O2 separation and the phenol hydrogen locations in the final Fourier difference maps.[20] Within the lattice, the molecule is well-isolated with no strong intermolecular interactions.

The interaction of the ligand dianion with alkali metal cations is illustrated in the structure of the disodium biphenoxide salt, crystallized as the THF solvate, $[Na(THF)_2]_2[^{TPS}LO_2]$ ((THF)$_4$[**3**]) (Figure 2, Table 2). The net molecular structure tends toward C_2 symmetry. The biphenoxide ligand serves as a κ^2-chelate to both sodium countercations, with the irregular coordination sphere of each cation completed by two terminal THF ligands and by a distant, weak interaction with the proximal ipso carbon of the biphenoxide backbone. The steric protection afforded by the triphenylsilyl groups presumably deters further aggregation to form cation-bridged oligomers or polymers. We are unaware of any other crystallographically characterized alkali metal/2,2′-biaryloxide structure.[21]

Table 2. Selected Interatomic Distances and Angles in $[Na(THF)_2]_2(^{TPS}LO_2)$ ([**3**](THF)$_4$)

Na(1)−O(1)	2.334(4)	Na(2)−O(1)	2.231(4)
Na(1)−O(2)	2.286(4)	Na(2)−O(2)	2.313(4)
Na(1)−O(3)	2.315(4)	Na(2)−O(5)/O(5A)[a]	2.40(1)/2.281(9)
Na(1)−O(4)	2.309(5)	Na(2)−O(6)	2.315(5)
Na(1)···C(12)	2.775(5)	Na(2)···C(22)	2.680(6)
Na(1)···Na(2)	3.114(3)		

O(1)−Na(1)−O(2)	76.5(1)	O(1)−Na(2)−O(2)	78.0(1)
O(1)−Na(1)−O(3)	143.3(2)	O(1)−Na(2)−O(5/5A)[a]	84.1(3)/95.6(3)
O(1)−Na(1)−O(4)	126.6(2)	O(1)−Na(2)−O(6)	107.4(2)
O(2)−Na(1)−O(3)	98.7(2)	O(2)−Na(2)−O(5/5A)[a]	101.9(4)/123.6(3)
O(2)−Na(1)−O(4)	106.5(2)	O(2)−Na(2)−O(6)	130.5(2)
O(3)−Na(1)−O(4)	90.0(2)	O(5/5A)[a]−Na(2)−O(6)	127.5(4)/105.1(3)

C(11−16)/C(21−26)[b]	50.2(2)

[a] O(5) and O(5A) are separate components of a disordered THF molecule. [b] Biphenyl torsion, as defined by the dihedral angle between the two phenyl ring planes.

(b) 4-Coordinate Complexes. The structures of the bipyridyl (**6**) and bis(THF) (**8**, **9**) complexes are shown in Figure 3, with selected metrical parameters listed in Table 3. Not presented here is the structure of the bis(pyridine) adduct **5**, which was solved but not refined to completion because of extensive disorder within a large asymmetric unit (4 independent molecules with 260 non-hydrogen atoms total, not including disordered components).[22] This structure determination, nevertheless, was sufficient to verify that compound **5** shares the same basic geometric features as the related ferrous complexes **6** and **8**.

The 4-coordinate ferrous complexes adopt distorted tetrahedral coordination geometries with idealized C_2 point symmetry. The metal−ligand distances are typical for high-spin, 4-coordinate Fe(II).[23] Significant departures from regular tetrahedral geometries are evident in the dihedral angle between the O−Fe−O and the A1−Fe−A2 planes (53.5(1)° and 49.1(1)° for complexes **6** and **8**, respectively, vs 90° for a regular tetrahedron; A1, A2 = bipy/THF coligand donor atoms). These geometry distortions arise from the frontal steric projection of the triphenylsilyl substituents, which skews the two remaining ligand positions away from the regular tetrahedral vertexes.

A skew distortion is also obvious in the structure of chromous complex **9** (O−Cr−O/A1−Cr−A2 dihedral: 24.4(2)°). As a high-spin, 4-coordinate, d^4 metal ion, the Cr(II) center should prefer a square planar geometry,[24] but the

(20) The phenol hydrogens were not directly refined in the structure, but treated using an idealized riding model (see Supporting Information).

(21) Inclusion compounds of 1,1′-bi-2-naphthol with alkali metal hydroxides have been structurally characterized; while it seems likely that the binaphthol hydroxyls are deprotonated in these structures, the diffraction data was of limited resolution and atomic details were not presented: Toda, F.; Tanaka, K.; Wong, M. C.; Mak, T. C. W. *Chem. Lett.* **1987**, 2069.

(22) Crystal parameters for $(^{TPS}LO_2)Fe(py)_2$ (**5**): space group $P\bar{1}$ (No. 2), $Z = 8$, $a = 20.3766(6)$ Å, $b = 22.6822(9)$ Å, $c = 23.9322(9)$ Å, $\alpha = 109.583(1)°$, $\beta = 94.799(1)°$, $\gamma = 112.714(1)°$, $V = 9319.7(6)$ Å^3, temp = 200(2) K.

(23) Orpen, G. A.; Brammer, L.; Allen, F. H.; Kennard, O.; Watson, D. G.; Taylor, R. *J. Chem. Soc., Dalton Trans.* **1989**, S1.

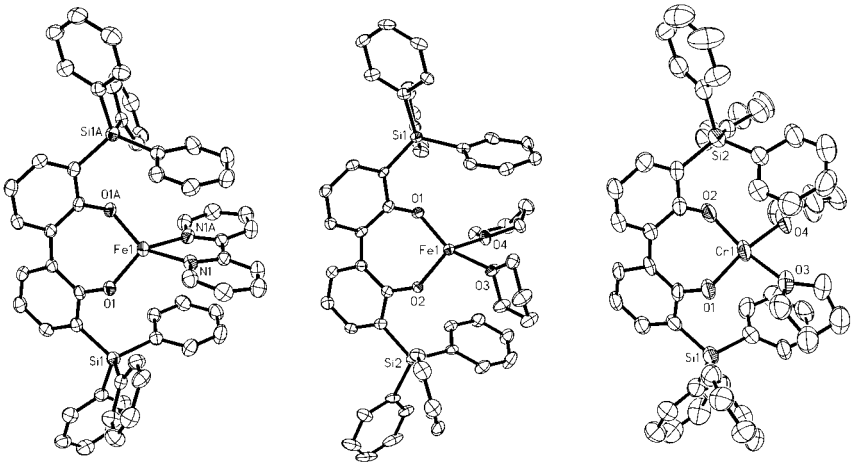

Figure 3. Structures of ($^{TPS}LO_2$)Fe(bipy) (**6**, left) and ($^{TPS}LO_2$)M(THF)$_2$ (M = Fe/Cr: **8**/**9**, center/right) with thermal ellipsoids (50% probability level) and selected atom labels; hydrogen atoms are not shown. For **6**, atoms with labels ending in "A" are generated by a crystallographic 2-fold axis. To allow geometry comparison, all three structures are presented using the same orientation relative to their common O(1)−M−(O1A/O2) planes.

Table 3. Selected Interatomic Distances (Å) and Angles (deg) in ($^{TPS}LO_2$)Fe(bipy) (**6**) and ($^{TPS}LO_2$)M(THF)$_2$ (M = Fe/Cr: **8**/**9**)[a]

	6	**8**	**9**
M(1)−O(1)	1.909(2)	1.903(2)	1.944(5)
M(1)−O(2)		1.915(2)	1.933(5)
M(1)−A1	2.129(2)	2.081(2)	2.053(6)
M(1)−A2		2.064(2)	2.069(5)
O(1)−M(1)−O(*a*)	102.0(1)	102.65(9)	96.2(2)
O(1)−M(1)−A1	102.15(8)	150.17(8)	90.4(2)
O(1)−M(1)−A2	141.32(8)	97.23(9)	160.7(2)
O(*a*)−M(1)−A1		95.24(8)	163.4(2)
O(*a*)−M(1)−A2		138.27(8)	90.4(2)
A1−M(1)−A2	76.1(1)	84.46(9)	88.3(2)
biphenyl torsion[b]	50.07(6)	54.22(8)	52.3(2)

[a] For **6**: A1 = N(1), A2 = N(1A), *a* = 1a; for **8** and **9**: A1 = O(3), A2 = O(4), *a* = 2. [b] Defined by the dihedral angle between the two phenyl ring planes, C(11−16)/C(11A−16A) (for **6**) or C(11−16)/C(21−26) (for **8** and **9**).

hindered biphenoxide ligand again forces a marked deformation away from the ideal. The metrical details of the coordination sphere are otherwise unexceptional.[23]

(c) [Fe(μ-$^{TPS}LO_2$)]$_2$ Dimer. The structure of dimer **4** approaches overall C_2 symmetry, with the paired iron centers and biphenoxide ligands interrelated through an approximate central rotational axis (Figure 4, Table 4; for clarity, a stereoview is provided as Figure 5). The biphenoxide ligation exhibits an unanticipated coordination mode, providing one terminal phenoxide donor, one bridging phenoxide, and a weak interaction from a pendant phenyl group of one silyl substituent; the ligand thereby serves as a strongly bound chelate to one iron (via both aryloxide donors) and a weaker chelate to the other (via a bridging aryloxide and the remote ring interaction). Each ferrous center adopts a distorted pseudo-4-coordinate geometry with three Fe−OAr bonds (Ar = aryl) and a "vacant" coordination site directed toward the π-face of a silylphenyl ring; the iron geometry is pyramidalized toward the remote phenyl ring and is best described as a flattened tetrahedral environment. The aryl ring interaction is asymmetric: the Fe···PhSi contact is closest to the 2-carbon, with the next nearest ring position (the 1-carbon) ca. 0.2 Å more distant. The Fe−OAr bond lengths are comparable to those of 4-coordinate high-spin Fe(II),[23] while the remote Fe−phenyl contacts, though longer than bonds found in arene complexes of Fe(II) (ca. 2.01 Å),[23] are much shorter than the sum of the van der Waals radius of an aryl carbon atom (estimated 1.7 Å)[24] and the metallic radius of iron (estimated 1.2 Å).[25] Similar weak aromatic donor

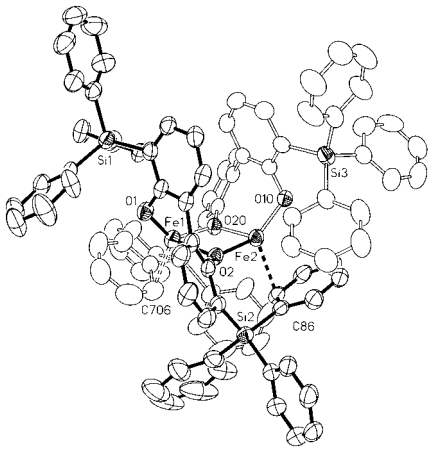

Figure 4. Structure of [Fe(μ-$^{TPS}LO_2$)]$_2$ (**4**) with thermal ellipsoids (50% probability level) and selected atom labels; hydrogen atoms are not shown. For clarity, the two independent biphenoxide ligands are differentiated using solid and hollow bonds.

Table 4. Selected Interatomic Distances and Angles in [Fe(μ-$^{TPS}LO_2$)]$_2$ (**4**)

Fe(1)−O(1)	1.870(2)	Fe(2)−O(10)	1.875(2)
Fe(1)−O(2)	2.085(2)	Fe(2)−O(20)	2.085(2)
Fe(1)−O(20)	1.996(2)	Fe(2)−O(2)	1.953(2)
Fe(1)−C(706)	2.468(4)	Fe(2)−C(86)	2.419(3)
O(1)−Fe(1)−O(2)	100.00(9)	O(10)−Fe(2)−O(20)	99.24(9)
O(1)−Fe(1)−O(20)	129.8(1)	O(10)−Fe(2)−O(2)	145.6(1)
O(1)−Fe(1)−C(706)	128.5(1)	O(10)−Fe(2)−C(86)	105.3(1)
O(2)−Fe(1)−O(20)	78.52(9)	O(20)−Fe(2)−O(2)	79.50(9)
O(2)−Fe(1)−C(706)	105.2(1)	O(20)−Fe(2)−C(86)	119.0(1)
O(20)−Fe(1)−C(706)	99.1(1)	O(2)−Fe(2)−C(86)	94.0(1)
C(11−16)/C(21−26)[a]	61.8(1)	C(31−36)/C(41−46)[a]	59.4(1)

[a] Biphenyl torsion, as defined by the dihedral angle between the two phenyl ring planes.

(24) Hermes, A. R.; Morris, R. J.; Girolami, G. S. *Organometallics* **1988**, *7*, 2372 and examples cited therein.

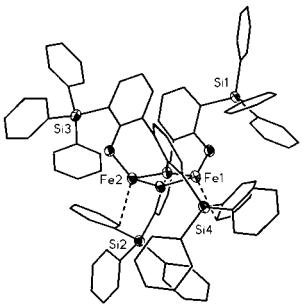

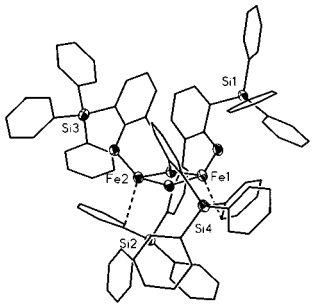

Figure 5. Stereoview of $[Fe(\mu\text{-}^{TPS}LO_2)]_2$ (**4**).

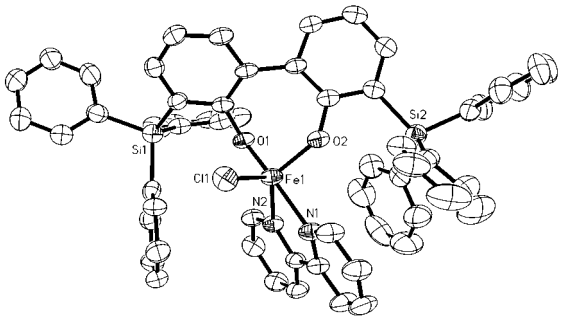

Figure 6. Structure of ($^{TPS}LO_2$)FeCl(bipy) (**10**) with thermal ellipsoids (50% probability level) and selected atom labels; hydrogen atoms are not shown.

interactions have been documented in 3d complexes of monodentate hindered arylchalcogenide ligands with *o*-aryl substituents.[26,27]

(d) 5- and 6-Coordinate Complexes. Ferric complex **10** assumes a 5-coordinate geometry intermediate between square pyramidal and trigonal bipyramidal (Figure 6, Table 5). As is the case for the ferrous bipyridyl complex **6**, the bipyridyl ligand is sandwiched within a cleft created by flanking triphenylsilyl substituents; the fifth ligand position occupied by chloride is exposed and directed away from this shielded pocket. Metal−ligand bond distances are consistent with expected values for a high-spin ferric complex.[23]

The 6-coordinate isonitrile complex **7** possesses a regular cis-octahedral stereochemistry (Figure 7, Table 5). To our knowledge, only two $[M(OR)_2(CNR')_4]^z$ structures have been reported previously.[28] One, with M = Mo(IV) and unhindered, monodentate ligands, adopts a trans-octahedral geometry.[28a] The other, with M = W(II), assumes a markedly distorted 6-coordinate cis geometry that originates from the steric influence of hindered, conformationally constrained monodentate aryloxide ligands.[28b] In contrast, for **7**, the

Table 5. Selected Interatomic Distances (Å) and Angles (deg) in ($^{TPS}LO_2$)FeCl(bipy) (**10**) and ($^{TPS}LO_2$)Fe(CNXy)$_4$ (**7**)

10		**7**	
Fe(1)−O(1)	1.905(2)	Fe(1)−O(1)	1.982(2)
Fe(1)−O(2)	1.847(2)	Fe(1)−O(2)	1.971(2)
Fe(1)−N(1)	2.146(3)	Fe(1)−C(1)	1.858(4)
Fe(1)−N(2)	2.144(3)	Fe(1)−C(2)	1.845(4)
Fe(1)−Cl(1)	2.249(1)	Fe(1)−C(3)	1.886(4)
		Fe(1)−C(4)	1.895(4)
O(1)−Fe(1)−O(2)	96.90(9)	O(1)−Fe(1)−O(2)	95.64(8)
O(1)−Fe(1)−N(1)	159.7(1)	O(1)−Fe(1)−C(1)	173.2(1)
O(1)−Fe(1)−N(2)	87.1(1)	O(1)−Fe(1)−C(2)	89.9(1)
O(1)−Fe(1)−Cl(1)	106.2(8)	O(1)−Fe(1)−C(3)	94.9(1)
O(2)−Fe(1)−N(1)	88.9(1)	O(1)−Fe(1)−C(4)	81.1(1)
O(2)−Fe(1)−N(2)	125.2(1)	O(2)−Fe(1)−C(1)	88.7(1)
O(2)−Fe(1)−Cl(1)	105.93(8)	O(2)−Fe(1)−C(2)	174.0(1)
N(1)−Fe(1)−N(2)	73.8(1)	O(2)−Fe(1)−C(3)	83.8(1)
N(1)−Fe(1)−Cl(1)	90.73(9)	O(2)−Fe(1)−C(4)	91.5(1)
N(2)−Fe(1)−Cl(1)	125.32(8)	C(1)−Fe(1)−C(2)	86.00(1)
		C(1)−Fe(1)−C(3)	90.7(1)
		C(1)−Fe(1)−C(4)	93.7(1)
		C(2)−Fe(1)−C(3)	93.5(1)
		C(2)−Fe(1)−C(4)	91.6(1)
		C(3)−Fe(1)−C(4)	173.5(1)
C(11−16)/C(21−16)[a]	48.50(8)	C(11−16)/C(21−16)[a]	51.2(1)

[a] Biphenyl torsion, as defined by the dihedral angle between the two phenyl ring planes.

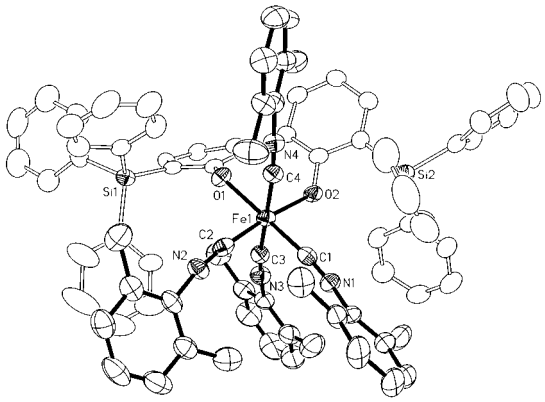

Figure 7. Structure of ($^{TPS}LO_2$)Fe(CNXy)$_4$ (**7**) with thermal ellipsoids (50% probability level) and selected atom labels; hydrogen atoms are not shown. For clarity, the biphenoxide chelate is depicted with hollow bonds.

planar aryl substituents of the isonitrile ligands interleave with each other and with the triphenylsilyl substituents to allow the complex to attain a relatively undistorted octahedral coordination geometry. The Fe−CNR distances are within the expected range for Fe(II);[23] the isonitriles positioned trans to each other show somewhat longer metal−ligand separations (ca. 0.04 Å) than the two bound trans to the aryloxides,

(25) Pauling, L. *The Nature of the Chemical Bond*, 3rd ed.; Cornell University Press: Ithaca, NY, 1960.
(26) (a) Ruhlandt-Senge, K.; Power, P. P. *Bull. Soc. Chim. Fr.* **1992**, *129*, 594. (b) Ellison, J. J.; Ruhlandt-Senge, K.; Power, P. P. *Angew. Chem., Int. Ed. Engl.* **1994**, *33*, 1178. (c) Ellison, J. J.; Power, P. P. *Inorg. Chem.* **1994**, *33*, 4231. (d) Ellison, J. J.; Ruhlandt-Senge, K.; Hope, H. H.; Power, P. P. *Inorg. Chem.* **1995**, *34*, 49. (e) Hauptmann, R.; Kliss, R.; Henkel, G. *Angew. Chem., Int. Ed.* **1999**, *38*, 377.
(27) Stronger interactions with *o*-aryl substituents of monodentate arylthiolate ligands have been observed for 4d metal centers: (a) Dilworth, J. R.; Zheng, Y.; Lu, S.; Wu, Q. *Inorg. Chim. Acta* **1992**, *194*, 99. (b) Buyuktas, B. S.; Olmstead, M. M.; Power, P. P. *Chem. Commun.* **1998**, 1689.
(28) (a) Isovitsch, R. A.; Beadle, A. S.; Fronczek, F. R.; Maverick, A. W. *Inorg. Chem.* **1998**, *37*, 4258. (b) Lockwood, M. A.; Fanwick, P. E.; Rothwell, I. P. *Organometallics* **1997**, *16*, 3574.

due presumably to the mutual, opposing trans influences (structural trans effects) for the former.[29] The Fe−OAr distances are notably longer than those found in the high-spin iron complexes **4**, **6**, **8**, and **10**. While structurally characterized examples of low-spin Fe(II)−aryloxide species are rare and do not offer an adequate basis for distance comparison,[30] the long Fe−OAr separations are unusual given that low-spin, 6-coordinate Fe(II) has an ionic radius (0.61 Å) between that of high-spin, 4-coordinate Fe(II) (0.63 Å) and that of 5-coordinate Fe(III) (0.58 Å).[31] The isonitrile ligands trans to the aryloxides may account for some of the bond lengthening, although isonitriles are generally held to exert only a modest trans influence;[29] the increased steric congestion associated with a 6-coordinate metal environment may be the other contributing factor for the longer Fe−OAr distances in **7**.

Discussion

3,3′-Bis(triphenylsilyl)biphenoxide as a Geometry-Constraining Ligand. A survey[31] of the Cambridge Crystallographic Database[33] shows biaryloxides as flexible ligands compatible with typical 4-, 5-, and 6-coordinate transition metal geometries.[34] Biaryloxide chelates display the full range of bite angles needed to bridge adjacent ligand sites in all of these environments, from the ubiquitous right angles found in octahedral, square pyramidal, trigonal bipyramidal, and square planar complexes to the expanded angles associated with tetrahedral metal centers (Figure 8). Backside steric encumbrance, present in 1,1′-binaphthyl and 6,6′-dimethylbiphenyl ligand backbones, affects chelate structure by increasing torsion at the biaryl linkage (Figure 8), but has no apparent influence on bite angle. Although increases in aryl−aryl torsion should expand chelate bite angles, the difference between hindered and unhindered dihedral angles for known ligands appears insufficient[35] to override other compensatory effects; indeed, the most acute bite angles (80−88°) are confined counterintuitively to complexes of biaryloxides with backside hindrance.

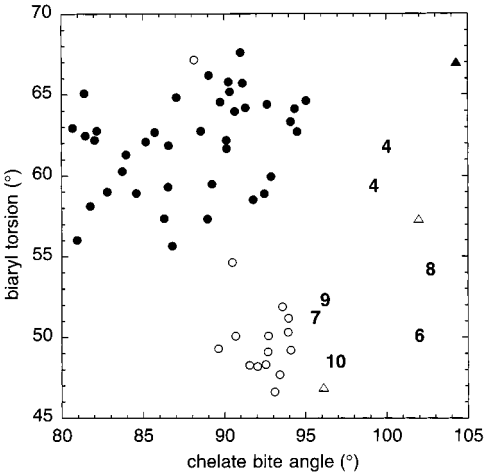

Figure 8. Plot of biaryl torsion vs chelate bite angle for biaryloxide chelate ligands in transition metal complexes (38 unique structures with 64 observations,[32] excluding 1 outlier[35]); biaryl torsion is defined as the dihedral angle between aryl ring planes. Entries are subdivided between tetrahedral, 4-coordinate species (triangles) and complexes with other geometries (circles), and between biaryloxides with backside steric hindrance (solid) and those without (hollow); entries for complexes reported in this work are designated by compound number (**4**, **6**, **7**, **8**, **9**, **10**).

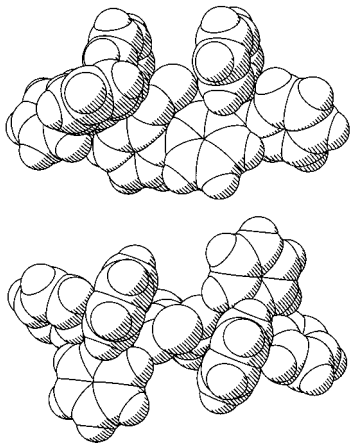

Figure 9. Space-filling representations of the [(^{TPS}LO$_2$)M] fragment as viewed from the front (bottom) and rotated 90° lengthwise (top). The relevant portion of complex **6** is used for the model; C, H, and O atoms are depicted at full van der Waals radii (1.7, 1.2, and 1.4 Å, respectively),[25] while Si and M atoms are shown with arbitrary radii (1.7 and 1.5 Å, respectively).

Molecular modeling suggests that, for small metal ions (3d elements or lighter) with no electronic structure preference, the frontside steric demand of the triphenylsilyl-substituted biaryloxide ligands will favor the formation of mononuclear, monochelate complexes of distorted tetrahedral metal geometry.[36] The structures of the 4-coordinate ferrous complexes demonstrate this coordination mode. Space-filling representations of the [(^{TPS}LO$_2$)Fe] fragment of complex **6** illustrate the steric extent of the bound hindered biphenoxide (Figure 9): the triphenylsilyl substituents project forward over the metal center, bracketing the remaining coordination sites to form a pronounced C_2-symmetric binding cleft. The prominent skew distortions away from tetrahedral and square

(29) Coe, B. J.; Glenwright, S. J. *Coord. Chem. Rev.* **2000**, *203*, 5.
(30) We know of only three structurally characterized low-spin Fe(II) aryloxide complexes; two of these involve κ^2-2-nitrosophenoxide chelation, which may not be metrically comparable to simple aryloxide ligation, and all three structures are marked by limited diffraction data, high final *R* factors (>9% in all cases), and large estimated standard deviations for interatomic distances (ca. 0.01−0.03 Å for Fe−O bonds): (a) De Sanctis, S. C.; Hodgkin, D. C. *Proc. R. Soc. London B* **1973**, *184*, 121. (b) De Sanctis, Grdenic, D.; Taylor, N.; Hodgkin, D. C. *Proc. R. Soc. London B* **1973**, *184*, 137. (c) Boinnard, D.; Bousseksou, A.; Dworking, A.; Savariault, J.-M.; Varret, F.; Tuchagues, J.-P. *Inorg. Chem.* **1994**, *33*, 271.
(31) Shannon, R. D. *Acta Crystallogr.* **1976**, *A32*, 751.
(32) A complete listing of search results (structures, references, relevant metrics) is provided as Supporting Information.
(33) (a) *Cambridge Structural Database*, version 5.21; Cambridge University: Cambridge, England, April 2001. (b) Allen, F. H.; Kennard, O. *Chem. Des. Autom. News* **1993**, *8*, 31.
(34) The coordinative and conformational flexibility of the binaphthoxide ligand was also noted in an earlier structural analysis: Boyle, T. J.; Barnes, D. L.; Heppert, J. A.; Morales, L.; Takusagawa, F.; Connolly, J. W. *Organometallics* **1992**, *11*, 1112.
(35) The excluded outlier belongs to a tetrahedral Mo(VI) complex with a biaryloxide chelate that spans a remarkable 127.0° bite angle; a substantial biaryl torsion of 82.6° is necessary to support this wide bite angle: Alexander, J. B.; La, D. S.; Cefalo, D. R.; Hoveyda, A. H.; Schrock, R. R. *J. Am. Chem. Soc.* **1998**, *120*, 4041.
(36) Most[5−10] of the aforementioned reactivity studies involving the binaphthoxide homologue were conducted and interpreted with this structural model in mind.

Table 6. Distortional Parameters[a] for the Biphenyl Rings in $^{TPS}L(OH)_2$ (**1**), ($^{TPS}LO_2$)Fe(bipy) (**6**), ($^{TPS}LO_2$)M(THF)$_2$ (M = Fe/Cr: **8/9**), [Fe(μ-$^{TPS}LO_2$)]$_2$ (**4**), ($^{TPS}LO_2$)FeCl(bipy) (**10**), and ($^{TPS}LO_2$)Fe(CNXy)$_4$ (**7**)

					4			
	1	**6**	**8**	**9**	ligand 1	ligand 2	**10**	**7**
rms deviation[b] from phenyl plane,[c] Å	0.005, 0.004	0.001	0.019, 0.019	0.003, 0.012	0.029, 0.023	0.016, 0.016	0.043, 0.013	0.048, 0.028
C1′ displacement from phenyl plane,[c] Å	0.100(4), 0.028(4)	0.097(5)	0.150(5), 0.244(5)	0.00(1), 0.12(1)	0.283(6), 0.178(5)	0.170(5), 0.186(5)	0.335(5), 0.018(5)	0.399(5), 0.265(5)
C1′−C1···C4 para bend,[d] deg	176.3(2), 177.3(2)	173.91(9)	172.8(2), 170.6(2)	174.8(5), 174.8(5)	169.7(3), 172.8(3)	172.5(3), 172.4(2)	168.8(2), 173.9(3)	166.5(2), 169.8(2)
O displacement from phenyl plane,[c] Å	0.029(4), 0.043(4)	0.033(3)	0.061(4), 0.063(4)	0.020(9), 0.01(1)	0.072(5), 0.128(5)	0.053(5), 0.077(4)	0.247(4), 0.129(4)	0.198(4), 0.058(4)
O−C2···C5 para bend,[d] deg	178.1(2), 178.2(2)	177.3(2)	177.5(2), 177.1(2)	177.6(5), 177.7(6)	178.0(3), 176.7(2)	178.4(3), 178.0(2)	172.8(2), 174.2(2)	178.9(2), 175.6(2)
Si displacement from phenyl plane,[c] Å	0.009(3), 0.027(4)	0.023(4)	0.212(4), 0.068(4)	0.079(9), 0.07(1)	0.610(5), 0.209(5)	0.354(5), 0.145(4)	0.475(4), 0.165(5)	0.238(4), 0.176(4)
Si−C3···C6 para bend,[d] deg	179.4(1), 179.2(1)	178.9(2)	174.4(2), 178.3(2)	177.6(4), 177.1(4)	162.1(2), 174.6(2)	169.7(2), 175.4(2)	167.1(2), 175.5(2)	174.1(2), 175.6(2)

[a] Positional ring notation: C1−C6 = phenyl carbon atoms, C1′ = carbon of the other phenyl ring bound to C1, O = phenoxy oxygen bound to C2, Si = silicon bound to C3. [b] Root-mean-square deviation for the least-squares fitted phenyl carbon atoms (C1−C6). [c] Perpendicular displacement from the fitted phenyl plane. [d] Para bend refers to the angle formed by the substituent and the phenyl para carbon with the ipso carbon as vertex.

planar geometries noted in complexes **6**, **8**, and **9** provide direct evidence of geometry-altering, nonbonded intramolecular contacts between the sterically demanding triphenylsilyl groups and the other components of the coordination sphere. Previous structurally characterized 4-coordinate biaryloxide complexes all employ less hindered chelates and consequently show little to no deformation of their coordination polyhedra.[37]

The structures of dimer **4**, 5-coordinate **10**, and 6-coordinate **7** establish that the [($^{TPS}LO_2$)M] environment, despite the steric demand of the triphenylsilyl substituents, also accommodates alternate, expanded coordination geometries with coligands of low steric demand. In comparing the structural parameters of these species against those of the 4-coordinate complexes, we find that the biphenoxide chelate has little effect on the higher coordinate, mononuclear metal environments (with the possible exception of the aforementioned long Fe−OAr distances in isonitrile complex **7**), but does create an irregular metal geometry on dimer **4** due to its unusual binding mode. The chelate itself adapts across the entire structural series by spanning a 7° spread of bite angles intermediate between perfect right and tetrahedral angles; the ordering of these angles is consistent with coordination geometry, with the sharpest angle occurring at the octahedral metal center and the widest angles at tetrahedral sites (see Tables 2−5 and Figure 8). The aryl−aryl dihedral angles lie within the range expected for torsionally unhindered biphenoxide chelates, with the exception of dimer **4** where the ligand bridging necessitates a larger, but unremarkable, biaryl twist.

The presence of a normal metal geometry in **7** and **9** does not imply the absence of steric conflict between the hindered chelate and the other ligands: the strain is manifested instead in the biphenoxide ligand itself. Structural analysis of the phenyl units in the ligand backbones reveals a systematic pattern of deformation from planar ideals, as measured by deviations in the six-carbon phenyl fragment, displacements of the phenyl substituents relative to the plane, and bend angles of these substituents through the ipso and para carbons of the phenyl ring (Table 6). Free biphenol **2**, whose structure is dictated by inherent preferences, a single internal hydrogen bond, and intramolecular packing forces, exhibits only minor fluctuations from planarity at the backbone phenyl sites. Relative to this "relaxed" reference structure, the 4-coordinate mononuclear complexes display comparable, slight ring distortions since chelate steric demands are satisfied by twisting the coordination polyhedra. The 5- and 6-coordinate species, however, are too crowded to relieve steric clashes through simple adjustment of metal geometry, and so reveal more obvious nonplanar deviations at the chelate backbone. Although these distortions are relatively modest when quantified as local metrical perturbations, they lead to significant gross changes when summed across the entire ligand framework. Superposition of the chelate structures against the free diol framework (Figure 10) provides a straightforward visual gauge of this overall distortion: as strain increases, so too does the deflection of the triphenylsilyl substituents away from the congested metal center. The structural overlays also reveal conformational changes at the triphenylsilyl propeller that become very prominent as crowding occurs; the magnitude of this response shows that the rotational freedom associated with the Si−C bonds significantly expands the stereochemical flexibility of the [($^{TPS}LO_2$)M] environment. All of these distortional and conformational effects also occur in dimer **4**, but arise in this case primarily from the exceptional binding mode of the bridging chelate.

Conclusion

3,3′-Bis(triphenylsilyl)-1,1′-bi-2-phenoxide is an easily synthesized, sterically demanding dianionic bidentate ligand of potential utility in applications requiring geometry constraint of reactive metal sites. As an ancillary ligand, this biaryloxide derivative forms crystalline complexes that undergo controlled solution chemistry even using low-coordinate, high-spin, exchange-labile metal centers. Our

(37) Skew angles (O−M−O/A1−M−A2 dihedral) for previously characterized, 4-coordinate biaryloxide complexes (9 entries, 18 observations) range from 85.2° to 87.4° in tetrahedral geometries and 0.3° to 6.8° for square planar centers; search results are provided as Supporting Information.

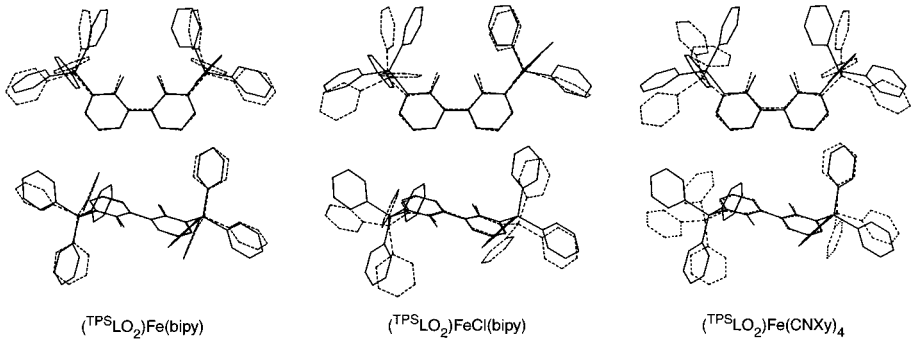

Figure 10. Superposition of biphenoxide chelate structures (dashed traces) in complexes **6** (left), **9** (center), and **7** (right) against the structure of the free diol **2** (solid traces) using least-squares fits of the biphenoxy backbones (O(1), C(11A−16A), O(1A/2), C(11A−16A)/(21−26)).

structural analysis reveals that the steric influence of the hindered chelate over the metal environment, while significant, is also compliant and moderated by deformational and conformational changes within the ligand itself. Although many of the ligand distortions noted in this study are intrinsic to the biaryloxy skeleton and thus difficult to control, the interplay of triphenylsilyl conformation with metal geometry and coligands suggests that further modification of this directing group can effectively enhance the stereochemical rigidity of the coordination sphere.

Experimental Section

General Considerations. Synthetic operations and physical measurements were conducted using protocols previously described.[3] Cr[N(SiMe$_3$)$_2$]$_2$(THF)$_2$ was prepared by modification of the literature procedure:[19a] commercial Na[N(SiMe$_3$)$_2$] was used instead of Li[N(SiMe$_3$)$_2$] generated in situ, and the reaction was stirred over a period of 24 h instead of 10 days before workup; yields for the modified synthesis were comparable to that reported for the original preparation. Pyridine was distilled from CaH_2 and stored over 4 Å molecular sieves under a pure dinitrogen atmosphere prior to use. Infrared spectra were recorded on a Nicolet 730 FTIR spectrometer.

2,2′-Dimethoxy-3,3′-bis(triphenylsilyl)-1,1′-biphenyl (1). To a rapidly stirred, fine suspension of 2,2′-dimethoxy-1,1′-biphenyl (20.0 g, 93.3 mmol) and TMEDA (42.3 mL, 280 mmol) in 500 mL of Et_2O at −78 °C was added dropwise 22.5 mL of a 10 M solution of *n*-butyllithium in hexanes (225 mmol). Stirring was continued for 8 h at room temperature, after which the reaction mixture was cooled to −5 °C and a solution of Ph_3SiCl (60.0 g, 203 mmol) in Et_2O (500 mL) introduced by cannula. The resulting mixture was stirred for 24 h at room temperature and then filtered to give an off-white precipitate, which was rinsed with Et_2O. The solid was redissolved in CH_2Cl_2 and filtered again to remove LiCl; solvent removal in vacuo, followed by recrystallization from CH_2Cl_2/Et_2O, yielded 17.5 g (26%) of pure bianisole **1** as a white microcrystalline solid. ^{1}H NMR (500 MHz, $CDCl_3$): δ 2.53 (s, OCH_3, 6H), 7.08 (t, J = 7.5 Hz, biphenyl, 2H), 7.23 (dd, J = 7.5, 1.5 Hz, biphenyl, 2H), 7.35 (m, $SiPh_3$, 12H), 7.40 (m, $SiPh_3$, 6H), 7.54 (dd, J = 7.5, 1.5 Hz, biphenyl, 2H), 7.64 (dd, J = 7.5, 1.5 Hz, $SiPh_3$, 12H). ^{13}C NMR (125 MHz, CDCl3): δ 59.2, 123.5, 127.8, 128.5, 129.4, 130.7, 134.4, 135.2, 136.7, 137.7, 163.3. MS (EI): *m*/*z* 730 [M^+, 31], 653 [$(M - C_6H_5)^+$, 45], 259 [$SiPh_3^+$, 100]. HRMS (EI): *m*/*z* 730.27308 [calcd M^+ for $C_{50}H_{42}O_2Si_2$, 730.27234].

3,3′-Bis(triphenylsilyl)-1,1′-bi-2-phenol (2, ^{TPS}L(OH)$_2$). BBr_3 (3.87 mL, 41.0 mmol) was added dropwise via gastight syringe to a stirred solution of bianisole **1** (15 g, 20.5 mmol) in 400 mL of CH_2Cl_2 at −78 °C. After being stirred for 6 h at room temperature, the yellow solution was treated with 500 mL of H_2O and then acidified with concentrated HCl, and more CH_2Cl_2 (300 mL) was added. The biphasic mixture was partitioned and the aqueous layer washed with CH_2Cl_2 (2 × 200 mL); all organic fractions were combined, washed with H_2O (500 mL), dried over Na_2SO_4, and reduced to dryness in vacuo. The resulting yellowish-white residue was redissolved in CH_2Cl_2 and the solution concentrated to give colorless microcrystals of biphenol **2**, which were isolated by filtration, rinsed with *n*-pentane, and dried in vacuo; the mother liquor was further concentrated and cooled to −20 °C to obtain a second crop. Combined yield: 7.2 g (50%). ^{1}H NMR (500 MHz, $CDCl_3$) δ 5.68 (s, OH, 2H), 7.06 (t, J = 7.5 Hz, biphenyl, 2H), 7.25 (m, biphenyl, 2H), 7.36 (t, J = 7.5 Hz, $SiPh_3$, 12H), 7.43 (m, biphenyl and $SiPh_3$, 8H), 7.62 (m, $SiPh_3$, 12H). ^{13}C NMR (125 MHz, $CDCl_3$): δ 121.1, 121.6, 124.5, 128.2, 129.9, 134.2, 134.21, 136.5, 138.9, 158.2. MS (EI): *m*/*z* 702 [M^+, 11], 624 [$(M - C_6H_6)^+$, 18], 547 [$(M - C_6H_6 - C_6H_5)^+$, 34], 469 [$(M - 2C_6H_6 - C_6H_5)^+$, 29], 391 [$(M - 3C_6H_6 - C_6H_5)^+$, 39], 259 [$SiPh_3^+$, 100]. HRMS (EI): *m*/*z* 702. 23875 [calcd M^+ for $C_{48}H_{36}O_2Si_2$, 702.24104].

Na$_2$(^{TPS}LO$_2$) (3). NaH (0.088 g, 3.67 mmol) was added in small portions to a rapidly stirred THF (150 mL) solution of biphenol **2** (1.00 g, 1.42 mmol). Stirring was maintained for 24 h, after which the mixture was filtered to remove excess NaH and evaporated in vacuo to give a white solid. The crude product was recrystallized from THF/*n*-pentane; rigorous drying of the microcrystals so obtained removed all cation-bound THF to give 0.700 g (66%) of the unsolvated disodium salt **3**. ^{1}H NMR (500 MHz, CD_3CN): δ 6.57 (t, J = 7.5 Hz, biphenyl), 6.86 (dd, J = 7.5, 1.5 Hz, biphenyl), 7.32 (m, $SiPh_3$, 9H), 7.45 (dd, J = 7.5, 1.5 Hz, biphenyl), 7.55 (m, $SiPh_3$, 6H). ^{13}C NMR (125 MHz, CD_3CN): δ 115.8, 121.9, 128.4, 129.7, 130.8, 134.1, 137.1, 137.2, 137.4, 138.2, 170.4.

[Fe(μ-^{TPS}LO$_2$)]$_2$ (4). A green solution of Fe[N(SiMe$_3$)$_2$]$_2$16 (0.350 g, 0.93 mmol) in benzene (1 mL) was added to a solution of biphenol **2** (0.500 g, 0.72 mmol) in benzene (5 mL), resulting in an instantaneous color change to yellow. The solution was stirred for 2 h and then layered with 2 vol equiv of *n*-pentane. The yellow crystalline blocks that grew overnight were collected by filtration, washed with *n*-pentane, and dried in vacuo to give 0.365 g (68%) of pure **4**. ^{1}H NMR (500 MHz, CD_2Cl_2): δ −63.47 (s, biphenyl, 2H), −31.73 (s, biphenyl, 2H), −8.19 (s, biphenyl, 2H), 2−6 (v br, $SiPh_3$, 30 H), 24.61 (s, biphenyl, 2H), 30.03 (s, biphenyl, 2H), 30.65 (s, biphenyl, 2H). Anal. Calcd for $C_{96}H_{72}O_4Si_4Fe_2$: C, 76.17; H, 4.79; Fe, 7.38. Found: C, 76.06; H, 4.99; Fe, 6.99.

(^{TPS}LO$_2$)Fe(py)$_2$ (5). A stirred solution of dimer **4** (0.100 g, 0.066 mmol) in 5 mL of CH_2Cl_2 was treated with pyridine (0.016 g, 0.202 mmol), resulting in an instantaneous color change to dark golden yellow. The reaction solution was stirred for 1 h and then

concentrated in vacuo. Vapor diffusion of several volume equivalents of *n*-pentane into this solution yielded green crystals, which were collected, washed with *n*-pentane, and dried in vacuo to give 0.085 g (70%) of complex **5**. ^{1}H NMR (500 MHz, CD_2Cl_2): δ −27.0 (s, biphenyl, 2H), 3.20 (br, $SiPh_3$, 12H), 4.45 (br, $SiPh_3$, 12H), 5.80 (br, $SiPh_3$, 6H), 10.1 (s, py, 2H), 26.0 (s, biphenyl, 2H), 29.5 (s, biphenyl, 2H), 46.4 (br, py, 4H). Anal. Calcd for $C_{58}H_{46}N_2O_2Si_2Fe$: C, 76.13; H, 5.07; N, 3.06; Fe, 6.10. Found: C, 76.35; H, 5.25; N, 3.20; Fe, 6.66.

(^{TPS}LO$_2$)Fe(bipy) (6). The preparative procedure for complex **5** was employed using 0.050 g (0.033 mmol) of **4**, 0.011 g (0.070 mmol) of 2,2′-bipyridyl, and 5 mL of CH_2Cl_2. The resulting dark red-brown solution was stirred for 2 h before concentration; vapor diffusion of Et_2O over 2 days yielded brown crystals of complex **6** (0.035 g, 62%). ^{1}H NMR (500 MHz, CD_2Cl_2): δ −23.28 (s, biphenyl, 2H), −7.74 (s, bipy, 2H), 0.5−4.0 (v br, $SiPh_3$), 4.0−7.0 (v br, $SiPh_3$), 23.82 (s, biphenyl, 2H), 28.79 (s, biphenyl, 2H), 62.43-(s, bipy, 2H), 85.52 (s, bipy, 2H). Anal. Calcd for $C_{53}H_{44}N_2O_2Si_2$-Fe: C, 74.63; H, 5.20; N, 3.28; Fe, 6.55. Found: C, 75.19; H, 4.95; N, 3.13; Fe, 7.08.

(^{TPS}LO$_2$)Fe(CNXy)$_4$ (7, Xy = 2,6-Xylyl). The preparative procedure for complex **5** was employed using 0.050 g (0.033 mmol) of **4**, 0.035 g (0.264 mmol) of 2,6-dimethylphenylisonitrile, and 5 mL of CH_2Cl_2. The resulting dark orange-red solution was stirred for 30 min before concentration; vapor diffusion of *n*-pentane over 1 h yielded orange-red microcrystals of complex **7** (0.073 g, 86%). ^{1}H NMR (500 MHz, C_6D_6): δ 1.47 (s, Me, 12H), 2.35 (s, Me, 12H), 6.47 (d, J = 7.5 Hz, ArH, 4 H), 6.62 (t, J = 7.5 Hz, ArH, 2H), 6.72−6.88 (m, ArH, 20H), 6.89−7.00 (m, ArH, 8 H), 7.45 (d, J = 7.5 Hz, ArH, 2 H), 7.85 (d, J = 6 Hz, ArH, 12H). IR (KBr): 2184 (w), 2145 (vs), 2127 (vs), 2105 (vs) (ν(NC)). Anal. Calcd for $C_{83}H_{72}N_4O_2Si_2Fe$: C, 78.73; H, 5.66; N, 4.37; Fe, 4.36. Found: C, 79.17; H, 5.83; N, 4.18; Fe, 4.71.

(^{TPS}LO$_2$)Fe(THF)$_2$ (8). $FeCl_2$ (0.085 g, 0.67 mmol) was added to a rapidly stirred THF (20 mL) solution of disodium biphenoxide salt **3** (0.500 g, 0.67 mmol), resulting in a dark blue-green solution color. The reaction mixture was stirred for 15 min, filtered to remove NaCl, and concentrated in vacuo to a minimal volume. Vapor diffusion of several volume equivalents of *n*-pentane over 6 h at room temperature gave blue-green crystalline blocks of complex **8**, which were collected, washed with *n*-pentane, and dried in vacuo (0.194 g, 35%). At room temperature, complex **8** is unstable both in solution (blue solutions decolorize within 24 h) and in the solid state; crystalline **8** was therefore stored at −30 °C to minimize decomposition. Dissolution of **8** in C_6D_6 gives a yellow solution color and ^{1}H NMR spectrum identical to that of **4**. Anal. Calcd for $C_{56}H_{52}O_4Si_2Fe$: C, 74.65; H, 5.82. Found: C, 70.57; H, 5.53. Unsatisfactory elemental analyses (multiple attempts) reflect sample decomposition at room temperature.

(^{TPS}LO$_2$)Cr(THF)$_2$ (9). A stirred violet solution of $Cr[N(SiMe_3)_2]_2$-$(THF)_2$[19] (0.044 g, 0.085 mmol) in toluene (5 mL) was treated with a solution of biphenol **2** (0.060 g, 0.085 mmol) in toluene (5 mL) to give an instantaneous solution color change to dark purple and the separation of purple microcrystals within 10 min. Stirring was continued for an additional 30 min, after which the purple microcrystalline precipitate was isolated by filtration, washed with *n*-pentane, and dried in vacuo to give 0.061 g (79%) of complex **10**. ^{1}H NMR (500 MHz, CD_2Cl_2): δ −6.20 (br, biphenyl), 1.20−9.80 (v br, SiPh3), 1.65 (br, THF), 3.85 (br, THF), 8.80 (br, biphenyl), 15.90 (br, biphenyl). Anal. Calcd for $C_{56}H_{52}O_4Si_2Cr$: C, 74.97; H, 5.84; Cr, 5.80. Found: C, 75.10; H, 6.06; Cr, 5.45.

(^{TPS}LO$_2$)FeCl(bipy) (10). $FeCl_3$ (0.045 g, 0.27 mmol) was added to a rapidly stirred solution of disodium biphenoxide **3** (0.200 g, 0.27 mmol) in THF (10 mL), producing a dark purple-red color. After the reaction mixture was stirred for 1 h, a solution of 2,2′-bipyridyl (0.042 g, 0.27 mmol) in 1 mL of THF was added to it, resulting in an opaque red-brown solution color. The mixture was stirred for an additional 12 h and then filtered to remove NaCl and evaporated in vacuo to afford a dark red-brown microcrystalline residue. This material was redissolved in a minimal amount of THF and the solution filtered again; vapor diffusion of Et_2O into the filtrate over 2 days gave very dark red (almost black) crystals of **10**, which were collected, washed with Et_2O, and dried in vacuo (0.050 g, 20%). Crystallizations were always accompanied by the deposition of limited amounts of unidentified red, insoluble powder in addition to crystalline **10**, even after successive recrystallizations; this may account for unsatisfactory elemental analyses (multiple attempts). ^{1}H NMR (500 MHz, CD_2Cl_2): δ 6.20−8.10 (v br). Anal. Calcd for $C_{58}H_{44}ClN_2O_2Si_2Fe$: C, 73.45; H, 4.68; N, 2.95; Fe, 5.89. Found: C, 75.91; H, 4.85; N, 3.22; Fe, 6.45.

X-ray Crystallography. Crystals suitable for single-crystal X-ray diffraction analysis were grown by room temperature vapor diffusion of benzene/*n*-pentane (for **2** and **4**·3C_6H_6, as colorless and yellow blocks, respectively), THF/*n*-pentane (for [**3**]$(THF)_4$·2THF and **8**, as colorless and green-blue blocks, respectively), CH_2-Cl_2/Et_2O (for **6**, as brown blocks, and **7**·(CH_2Cl_2/Et_2O), as orange-red needles), and THF/Et_2O (**10**·Et_2O·THF, as dark red blocks), and by vapor diffusion of CH_2Cl_2/Et_2O at −30 °C (**9**, as purple blocks).

General crystallographic procedures have been described elsewhere;[3] detailed information regarding specific structures and refinements in this work are provided as Supporting Information. The four cation-bound THF ligands in the structure of [**3**]$(THF)_4$ were each disordered over two site positions; the individual components were resolved and refined with appropriate restraints. Well-defined lattice-bound solvent molecules were identified and refined in the crystal structures of **4** (2 C_6H_6, one of which was constrained as a regular hexagon) and **10** (1 Et_2O). In addition, highly disordered solvent regions that could not be satisfactorily modeled were present in the lattices of **3** (2 THF), **4** (1 C_6H_6), **7** (compositional disorder of CH_2Cl_2/Et_2O), and **10** (1 THF); the SQUEEZE-BYPASS procedure[38] implemented in PLATON[39] was used to account for these residual electron densities.

Acknowledgment. The generous support of the Arnold and Mabel Beckman Foundation (Beckman Young Investigator Award) and the NSF (CAREER CHE-9984645) is gratefully acknowledged.

Supporting Information Available: Crystallographic data for compounds **2**, [**3**]$(THF)_4$·2THF, **4**·3C_6H_6, **6**, **7**·(CH_2Cl_2/Et_2O), **8**, **9**, and **10**·Et_2O·THF (CIF) and Cambridge Crystallographic Database search results (PDF). This material is available free of charge via the Internet at http://pubs.acs.org.

IC010909Y

(38) van der Sluis, P.; Spek, A. L. *Acta Crystallogr.* **1990**, *A46*, 194.
(39) (a) Spek, A. L. *PLATON. A multipurpose crystallographic tool*; Utrecht University: Utrecht, The Netherlands, 1999. (b) Spek, A. L. *Acta Crystallogr.* **1990**, *A46*, C34.